

## Article

# Integration of Indoor Air Quality Prediction into Healthy Building Design

Shen Yang <sup>1,\*</sup> , Sebastian Duque Mahecha <sup>2</sup> , Sergi Aguacil Moreno <sup>2</sup>  and Dusan Licina <sup>1</sup> 

<sup>1</sup> Human-Oriented Built Environment Lab, School of Architecture, Civil and Environmental Engineering, École Polytechnique Fédérale de Lausanne (EPFL), 1700 Fribourg, Switzerland; dusan.licina@epfl.ch

<sup>2</sup> Building2050 Group, School of Architecture, Civil and Environmental Engineering, École Polytechnique Fédérale de Lausanne (EPFL), 1700 Fribourg, Switzerland; sebastian.duque@epfl.ch (S.D.M.); sergi.aguacil@epfl.ch (S.A.M.)

\* Correspondence: shen.yang@epfl.ch

**Abstract:** Healthy building design is an emerging field of architecture and building engineering. Indoor air quality (IAQ) is an inevitable factor that should be considered in healthy building design due to its demonstrated links with human health and well-being. This paper proposes to integrate IAQ prediction into healthy building design by developing a simulation toolbox, termed i-IAQ, using MATLAB App Designer. Within the i-IAQ, users can input information of building layout and wall-openings and select air pollutant sources from the database. As an output, the toolbox simulates indoor levels of carbon dioxide (CO<sub>2</sub>), total volatile organic compounds (TVOC), inhalable particles (PM<sub>10</sub>), fine particles (PM<sub>2.5</sub>), nitrogen dioxide (NO<sub>2</sub>), and ozone (O<sub>3</sub>) during the occupied periods. Based on the simulation results, the toolbox also offers diagnosis and recommendations to improve the design. The accuracy of the toolbox was validated by a case study in an apartment where physical measurements of air pollutants took place. The results suggest that designers can integrate the i-IAQ toolbox in building design, so that the potential IAQ issues can be resolved at the early design stage at a low cost. The paper outcomes have the potential to pave a way towards more holistic healthy building design, and novel and cost-effective IAQ management.



**Citation:** Yang, S.; Mahecha, S.D.; Moreno, S.A.; Licina, D. Integration of Indoor Air Quality Prediction into Healthy Building Design. *Sustainability* **2022**, *14*, 7890. <https://doi.org/10.3390/su14137890>

Academic Editor: Alan Kabanshi

Received: 10 June 2022

Accepted: 26 June 2022

Published: 28 June 2022

**Publisher's Note:** MDPI stays neutral with regard to jurisdictional claims in published maps and institutional affiliations.



**Copyright:** © 2022 by the authors. Licensee MDPI, Basel, Switzerland. This article is an open access article distributed under the terms and conditions of the Creative Commons Attribution (CC BY) license (<https://creativecommons.org/licenses/by/4.0/>).

**Keywords:** building simulation; health and well-being; holistic and digital design; mass balance equation; toolbox

## 1. Introduction

Healthy buildings aim to support the physical, psychological, and social health and well-being of the occupants in the built environment [1,2]. According to the U.S. Green Building Council, healthy buildings are considered as the next generation of green building, which put more emphasis on human well-being and productivity [3,4]. Hence, healthy building design is an emerging need in the field of architecture and building engineering, especially in the face of increasing episodes of pandemics and climate events. The design of a healthy building requires comprehensive consideration of elements that are associated with human well-being and performance [5–8]. Among the factors, indoor air quality (IAQ) plays a crucial role in achieving healthy buildings [9].

Physical IAQ can be quantified using a matrix of concentrations of various indoor air pollutants. Exposure to indoor airborne contaminants is a long-standing issue directly linked with human health [10–12] and productivity outcomes [13,14]. A commonly used IAQ matrix can include gaseous and particulate pollutants, such as carbon dioxide (CO<sub>2</sub>), total volatile organic compounds (TVOC), inhalable particles (PM<sub>10</sub>), fine particles (PM<sub>2.5</sub>), nitrogen dioxide (NO<sub>2</sub>), and ozone (O<sub>3</sub>). Indoor CO<sub>2</sub> mainly originates from human exhalation and indoor combustion. Although the health effect of CO<sub>2</sub> within a common indoor concentration range remains unclear, the association between elevated CO<sub>2</sub> level and decreased human productivity and cognitive performance has been well documented [15–18].

Moreover, due to the direct link with the occupants' metabolism, indoor CO<sub>2</sub> level is also known as an indicator of the sufficiency of building ventilation [19,20]. TVOC is a sum of indoor gaseous organic chemicals that originate from various materials, personal care products, humans and their activities, and intrusion from outdoors [21–25]. Some of the chemicals are carcinogenic, such as benzene [26], while others are found to cause human irritation and respiratory symptoms [27,28]. Airborne particles are classified as carcinogenic to humans [29]. Exposure to PM<sub>10</sub> and PM<sub>2.5</sub> is also associated with respiratory and cardiopulmonary health [30,31]. Indoor particles can come from human-associated sources [32–34], indoor combustion [35], and outdoor penetration [36]. As an inorganic gaseous pollutant, NO<sub>2</sub> is significantly related to mortality and morbidity [37,38]. Indoor NO<sub>2</sub> can originate from outdoor intrusion and indoor gas cooking [39]. It also plays an important role in indoor chemistry [40]. Another inorganic gaseous pollutant, O<sub>3</sub>, also has adverse effects on human health [41,42]. O<sub>3</sub>-initiated chemistry has been found to alter indoor level and composition of VOCs and particles [43–45]. Indoor O<sub>3</sub> mainly comes from outdoor penetration [46], whereas some indoor electrical appliances can also contribute to building up indoor O<sub>3</sub> levels [47]. Represented by such a matrix of health-relevant air pollutants, IAQ is given a large weight in evaluating and certifying healthy buildings. The widely acknowledged healthy building rating tool, WELL, has given the priority to IAQ regarding air pollutant levels and IAQ management [48]. Therefore, IAQ is an inevitable factor that should be considered in healthy building design.

Current integration of IAQ into healthy building design, however, is disappointingly scarce, whereas the traditional IAQ control strategies are followed; IAQ management steps in after a building is constructed and occupied. Such post-intervention poses a risk for inadequate IAQ that requires tedious and expensive field commissioning, including multi-point measurements and investigations. Hence, the absence of involvement of IAQ in the building design stage leads not only to impaired health and productivity outcomes, but also to elevated costs of post-interventions. Although designers can refer to some general and qualitative guidelines, such as increasing ventilation and using low-emissive materials, they cannot ensure good IAQ. Even if some qualitative design approaches are implemented, they cannot match the emerging digitalized and parametric design trends of buildings.

The idea of this study is to integrate IAQ prediction into healthy building design to overcome the aforementioned shortages of the traditional strategies. IAQ is influenced by the interactions among outdoor air, indoor sources, ventilation, filtration, and occupants. The process is governed by fundamental mass transfer and material balance laws, which enables sufficiently accurate simulation of IAQ. Based on the quantitative prediction, designers can modify the design accordingly to achieve their IAQ goals, so that potential IAQ issues can be resolved at the very beginning (design) stage at the lowest costs. Recently, few studies have attempted to predict post-occupancy IAQ before the building is occupied [49]. Liang et al. [50], Chen et al. [51], and Lv et al. [52] focused on building renovation stage to simulate formaldehyde concentration after building renovation and proved that pre-intervention based on the simulation results can reduce health risks and management costs. D'Amico et al. also proposed to model VOC emissions from building materials in order to ensure healthy building design and integrated the VOC prediction with building information modelling (BIM) [53,54]. These studies, however, mainly focused on VOC emanated from materials while neglecting other potent indoor sources. In addition, to better represent IAQ and to propose pre-intervention methods, a comprehensive air pollutant matrix should be considered. It can not only better evaluate human exposure, but also elucidate which aspects of the design needs modification, as different pollutants correspond to distinct sources and management strategies.

This study aims to develop a simulation toolbox (i-IAQ) to predict post-occupancy IAQ at the building design stage. Based on the basic mass balance law, ventilation simulation, and indoor and outdoor pollution database, the i-IAQ toolbox can simulate post-occupancy indoor levels of CO<sub>2</sub>, TVOC, PM<sub>10</sub>, PM<sub>2.5</sub>, NO<sub>2</sub>, and O<sub>3</sub> at the design building stage. The

toolbox is also capable of offering diagnosis and suggestions for the design based on the simulation results. We performed a case study in an apartment to validate the reliability of the i-IAQ toolbox. The toolbox is currently developed targeting Switzerland, where the authors are located, but can also be applied to other countries and regions if the ambient weather and pollution databases get enriched. The project outcomes have the potential to pave a way towards novel and cost-effective IAQ management, and more holistic healthy building design.

## 2. Principle of the Toolbox

### 2.1. Overview of the Framework

Indoor air pollutant level is influenced by the interactions among outdoor air, indoor sources, ventilation, filtration, and occupants. The process is governed by mass balance laws, which enables accurate simulation of IAQ. For a building consisting of multiple rooms, the concentration of air pollutant  $k$  in room  $i$  can be described by Equation (1), which is as follows:

$$V_i \frac{dC_{i,k}}{dt} = \sum_j Q_{j,i} C_{j,k} + Q_{out,i} (\eta_{i,k} + p_{i,k}) C_{out,k} - Q_i C_{i,k} + E_{i,k} - (\beta_{i,k} V_i + CADR_{i,k}) C_{i,k} - S_{i,k} \quad (1)$$

where

$V_i$ : the volume of room  $i$ ;

$C_{i,k}$ : the concentration of air pollutant  $k$  in room  $i$ ;

$t$ : time;

$Q_{j,i}$ : the airflow rate from room  $j$  to room  $i$ ;

$C_{j,k}$ : the concentration of air pollutant  $k$  in room  $j$ ;

$Q_{out,i}$ : the airflow rate from outdoor to room  $i$ ;

$\eta_{i,k}$ : the one-pass filtration efficiency of air pollutant  $k$  from outdoor to room  $i$ , for mechanically ventilation equipped with air filters;

$p_{i,k}$ : the penetration coefficient of air pollutant  $k$  from outdoor to room  $i$  through openings;

$C_{out,k}$ : the outdoor concentration of air pollutant  $k$ ;

$Q_i$ : the sum of airflow rate from room  $i$ ;

$E_{i,k}$ : the emission rate of air pollutant  $k$  in room  $i$ ;

$\beta_{i,k}$ : the deposition rate of air pollutant  $k$  in room  $i$ ;

$CADR_{i,k}$ : the clean air delivery rate of air cleaners for air pollutant  $k$  in room  $i$ ;

$S_{i,k}$ : the strength of other sinks in room  $i$  for air pollutant  $k$ .

As observed from Equation (1), the factors governing the indoor air pollutant level can be categorized into building characteristics ( $V$ ,  $\eta$ , and  $p$ ); ventilation/infiltration ( $Q$ ); and indoor sources and sinks ( $E$ ,  $\beta$ ,  $CADR$ , and  $S$ ). An IAQ simulation toolbox needs to take these categorical factors into consideration to achieve reasonable IAQ prediction. Therefore, the framework of the i-IAQ toolbox can be summarized as shown in Figure 1, which also represents the workflow of the toolbox.

The i-IAQ toolbox contains four modules, namely, *Building*, *Airflow*, *Air pollutant*, and *Diagnosis* module. The *Building* module acquires the input of building information, including layout, size, location, type, and occupied period. Within the *Airflow* module, together with the ambient weather database, the toolbox simulates ventilation and infiltration of each room of the building. Based on the obtained airflow results, with additional input from the ambient pollution database and indoor source/sink database, the *Air pollutant* module calculates air pollutant concentrations in each room of the building. Finally, the *Diagnosis* module offers diagnosis and suggestions for the design based on the simulation results. The following sections describe each module in detail.

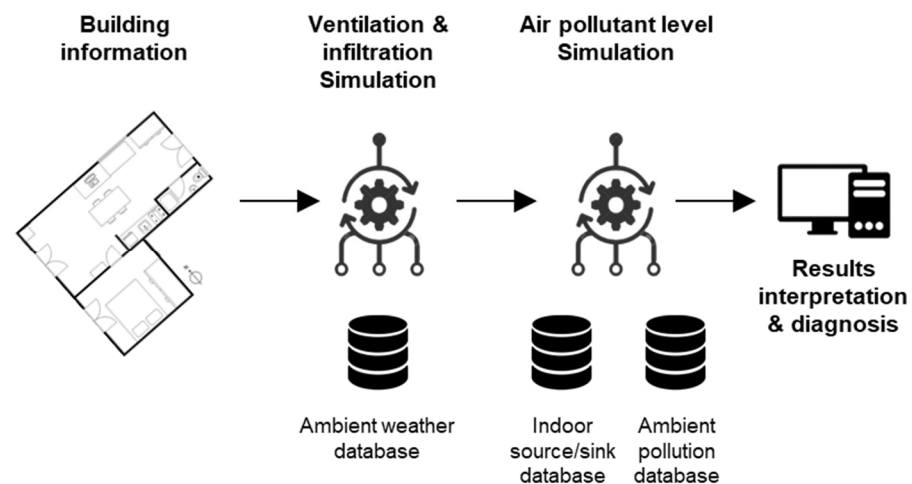


**Figure 1.** The framework of the i-IAQ toolbox.

## 2.2. Building Module

The *Building* module aims to collect basic information of the target building that is essential to perform ventilation/infiltration simulation and IAQ prediction. Building information should include the following: (1) layout, including information about number and size of rooms to be analyzed, including floor area, free height, and adjacency; (2) location, including the ambient weather and pollution data used in the *Airflow* and *Air pollutant* modules; (3) openings, including the location, size, height and direction of interior and exterior openings (windows and doors) enabling air exchanges between indoors and outdoors, as well as among rooms; (4) building type, including office or residential building, so that the toolbox can determine from predefined ventilation type and occupancy schedule of the building. Note that the selection of building type is optional, as users can customize the ventilation type and occupancy schedule. (6) Mechanical ventilation, including the designed outdoor air supply rate and the one-pass filtration efficiency for six air pollutants; (6) occupied period, to determine the starting date of IAQ prediction, as the toolbox runs a one-year simulation by default. The obtained data are then transferred to the *Airflow* module for ventilation/infiltration simulation of the target building.

## 2.3. Airflow Module

Generally, there are two approaches to perform airflow simulation in buildings, which are as follows: computational fluid dynamics (CFD) and multizone modelling, of which the former one can provide more accurate and refined characterization of the flow field but at considerably higher computational cost and time [55–57]. Therefore, aiming at rapid simulation with adequate accuracy, the *Airflow* module in the i-IAQ toolbox applies multizone modelling for ventilation and infiltration simulation of the target building. CONTAM is a widely used open-access multizone airflow modelling software developed by the US National Institute of Standards and Technology (NIST). The *Airflow* module of the i-IAQ toolbox principally follows the simulation setup of CONTAM as described below in brief, whereas details can be found in the CONTAM guide [58].

The toolbox considers each room and the outdoor space as an individual zone. Airflow between each adjacent zone is mainly driven by pressure difference, demonstrated by the following equation:

$$Q = C(\Delta P)^n \quad (2)$$

where  $Q$  represents airflow rate;  $C$  represents flow coefficient;  $\Delta P$  represents pressure difference between two zones; and  $n$  represents flow exponent. The flow coefficient  $C$  and flow exponent  $n$  depend on the property of airflow paths, i.e., openings of the target building. To simplify the settings, the i-IAQ toolbox adopts the leakage area model in CONTAM to simulate air infiltration when the openings are closed, of which the effective

leakage areas of building components are obtained from the ASHRAE Handbook [59]. When the windows or doors are open, the single opening with two-way flow model in CONTAM is applied to consider the potential two-way flow at the opening caused by air density and elevation differences. Details of these two models are described in the CONTAM guide [58]. In addition, for buildings equipped with mechanical ventilation systems, to simplify the simulation, the i-IAQ toolbox assumes an equal air supply and exhaust rate in each zone, which means that the simulation of natural ventilation and infiltration is independent from mechanical ventilation.

Considering the pressure deviation caused by temperature and wind,  $\Delta P$  can be further segregated into the following equation:

$$\Delta P = P_i - P_j + P_S + P_W \quad (3)$$

where  $P_i$  and  $P_j$  represent the total pressures at zone  $i$  and  $j$ ;  $P_S$  represents pressure difference due to density and elevation differences; and  $P_W$  represents pressure difference due to wind. The ambient weather is essential to calculate air exchange between indoor and outdoor space. The i-IAQ toolbox collects typical-year ambient weather data, including time stamp, dry-bulb air temperature, pressure, wind speed and wind direction, from an open source global database [60]. At present, the ambient weather database of the toolbox contains weather data of 25 major cities in Switzerland, which are the capitals of 25 Swiss cantons (Canton Appenzell Ausserrhoden was excluded due to lack of data).

The airflow across each zone is constrained by the following basic air mass balance equation:

$$\Delta F_i \equiv \rho_i Q_i - \sum_j \rho_j Q_{j,i} = 0 \quad (4)$$

$$\rho = \frac{PV}{RT} \quad (5)$$

where  $\Delta F_i$  is the mass imbalance rate of zone  $i$ ;  $\rho_i$  and  $\rho_j$  represent air density in zone  $i$  and  $j$ , which is determined by zone pressure ( $P$ ), zone volume ( $V$ ), zone temperature ( $T$ ), and gas constant for air ( $R$ ), as shown in Equation (5), for the ideal gas law. The airflow network of the target building can be obtained by solving Equations (2)–(5). The iteration procedure follows, (1) assuming  $P$  in each zone and calculating the mass imbalance rate  $\Delta F$  of each zone; (2) correcting  $P$  based on  $\Delta F$  in each zone and entering the next iteration; and (3) keeping iteration until the  $\Delta F$  of each zone is less than the acceptable error ( $\varepsilon = 10^{-8}$  kg/s), viewed as a convergence, and then the airflow rate between each adjacent zone can be obtained. Afterwards, the airflow matrix can be passed to the *Air pollutant* module for simulation of air pollutant concentrations.

#### 2.4. Air Pollutant Module

In addition to the airflow results from the *Airflow* module, the *Air pollutant* module also requires input from the ambient air pollution database and the indoor source/sink database to perform air pollutant level simulation.

The i-IAQ toolbox establishes the ambient air pollution database by collecting hourly mean atmospheric pollution data in the year 2019 (prior to the pandemic) from the National Air Pollution Monitoring Network (NABEL) in Switzerland [61]. The collected target air pollutants include non-methane VOCs (an approximation to TVOC),  $PM_{10}$ ,  $PM_{2.5}$ ,  $NO_2$ , and  $O_3$ . The NABEL has 16 monitoring locations, which is less than the number of major cities (25). Hence, for cities without a monitoring station, the ambient air pollution data are approximated using that from the closest station. The ambient  $CO_2$  concentration in the database is considered as constant at 420 ppm, as the level remains relatively stable within a year [62].

The indoor source/sink database is established by collecting indoor source and sink strength data reported in the literature [32,34,63–76]. As shown in Figure 2, the source/sink types collected in the database can be classified into the following five categories: human, furniture, building material, appliance, and other, which cover the commonly encountered

indoor air pollutant sources and sinks. At present, the database comprises 101 source/sink items. For each item, there are 20 columns of information stored, which can be aggregated into 3 categories of info (4 columns), emission per unit (10 columns), and deposition per unit (6 columns) (Figure 2). The info category contains miscellaneous data of the ID, name, note and unit of the item. The category of emission per unit collects emission rate data for the six air pollutants. Note that the TVOC emission rate data have four columns, considering that TVOC emissions from furniture and building materials are time-dependent, which can be described by various models. The database has three models (constant, exponential, and power models) [77] to characterize TVOC emission rate, indicated by the model *flag*,  $a_1$ ,  $a_2$ , and  $t_p$ , as shown in Equation (6), which is as follows:

$$E_{TVOC}(t) = \begin{cases} a_1, flag = 0 \\ a_1 e^{-0.5 \times (\ln(t/t_p)/a_2)^2}, flag = 1 \\ a_1 (\max(t, t_p))^{-a_2}, flag = 2 \end{cases} \quad (6)$$

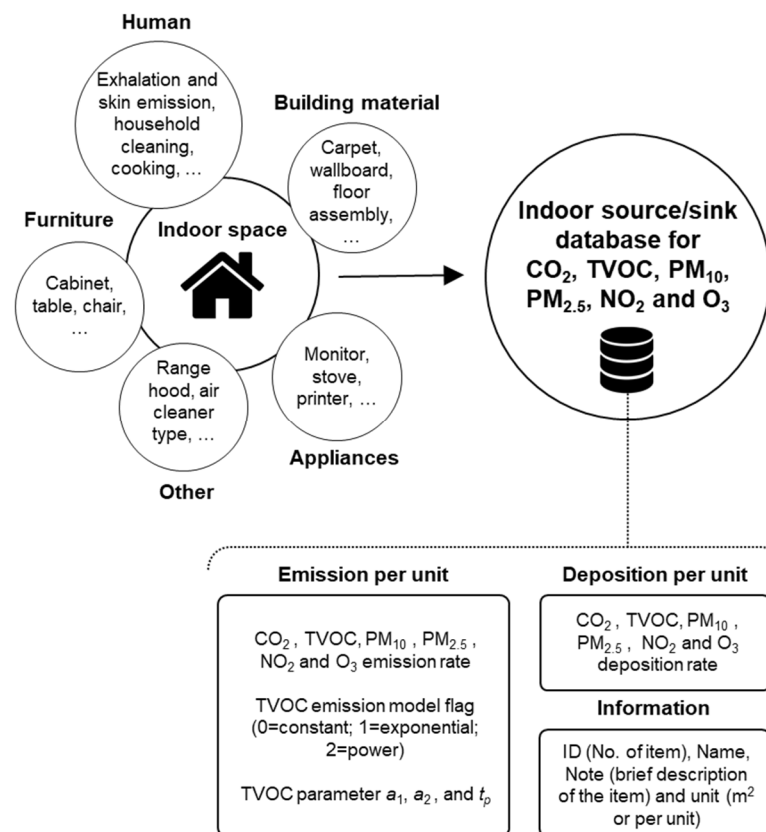


**Figure 2.** Structure of the indoor source/sink database for CO<sub>2</sub>, TVOC, PM<sub>10</sub>, PM<sub>2.5</sub>, NO<sub>2</sub>, and O<sub>3</sub> of the i-IAQ toolbox.

The category of deposition per unit stores deposition rates of six air pollutants of each item. It is not mutually exclusive for each item to be a source or a sink for IAQ simulation. For instance, humans are a potent source of indoor CO<sub>2</sub>, TVOC, PM<sub>10</sub>, and PM<sub>2.5</sub> [32,68,70], whereas they serve as a strong indoor sink of O<sub>3</sub> [71,78]. The comprehensive consideration of source and sink effect of occupants and building components can also be understood as a uniqueness and novelty of the database.

After gathering the inputs of airflow matrix, ambient air pollutant level, and indoor source/sink data, the *Air pollutant* module calculates multizone air pollutant concentrations

using the state-space method [79]. For the simulation of each air pollutant, Equation (1) can be rewritten as Equations (7) and (8), which are as follows:

$$\frac{dC}{dt} = AC + Bu \quad (7)$$

$$C = \begin{bmatrix} C_1 \\ \vdots \\ C_i \\ \vdots \\ C_N \end{bmatrix} \quad (8)$$

where  $C$  represents the state vector containing air pollutant concentrations in all rooms ( $1, \dots, N$ );  $A$  represents the system matrix relative to airflow and deposition, and the elements are shown in Equation (9);  $B$  is an identity matrix; and  $u$  represents the input vector containing intrusion of outdoor air pollutants, and indoor emissions and other sinks, of which the elements are calculated by Equation (10).

$$a_{ii} = -\frac{Q_i}{V_i} - \frac{\beta_i V_i + CADR_i}{V_i}; a_{ij} = \frac{Q_{j,i}}{V_i}; i, j = 1, \dots, N \quad (9)$$

$$u_i = \frac{E_i}{V_i} + \frac{Q_{out,i}(\eta_i + p_i)C_{out}}{V_i} - \frac{S_i}{V_i}; i = 1, \dots, N \quad (10)$$

Then, by discretizing Equation (7) using the time step  $\Delta t$ , the multizone air pollutant concentration  $C(t)$  can be obtained by the following equation:

$$C(t) = C(t - \Delta t) + \Delta t \times (A(t)C(t - \Delta t) + Bu(t)) \quad (11)$$

Afterwards, the simulation results of concentrations of six air pollutants in each room can be passed to the *Diagnosis* module for result interpretation and diagnosis.

### 2.5. Diagnosis Module

The *Diagnosis* module aims to deeply explore the simulation results of each room to provide suggestions for the design if there is a space for improvement. The first step of the diagnosis is to summarize the statistics of the air pollutant concentrations in each room and compare them with the set guideline values. The statistics mainly include calculating the maximum, mean, and median values of annual, 8-h average, and 24-h average air pollutant concentrations, which are parameters commonly adopted in the guidelines [48,80–82]. The default setting of the guideline values in the *Diagnosis* module is summarized in Table 1.

**Table 1.** The default guideline values [48,80–82] of air pollutant concentrations in the i-IAQ toolbox.

Parameter	CO <sub>2</sub> (ppm)	TVOC (µg/m <sup>3</sup> )	PM <sub>10</sub> (µg/m <sup>3</sup> )	PM <sub>2.5</sub> (µg/m <sup>3</sup> )	NO <sub>2</sub> (µg/m <sup>3</sup> )	O <sub>3</sub> (µg/m <sup>3</sup> )
8-h average	1200	-	-	-	-	100
24-h average	1000	500	45	15	25	-
Annual average	800	300	15	5	10	60

After obtaining the air pollutant concentration statistics and comparisons, the i-IAQ toolbox calculates a simple index,  $EXD_k$ , indicating the duration exceeding the guidelines of air pollutant  $k$  by

$$EXD_k = \frac{N_{exceeding,k}}{N_{total}} \times 100\% \quad (12)$$

where  $N_{exceeding,k}$  represents the number of data points that exceed the set guideline value of air pollutant  $k$ ; and  $N_{total}$  represents the number of total data points.

With the *EXD*, the toolbox runs an automatic diagnosis, of which the flow is illustrated in Figure 3 and described in detail as below.

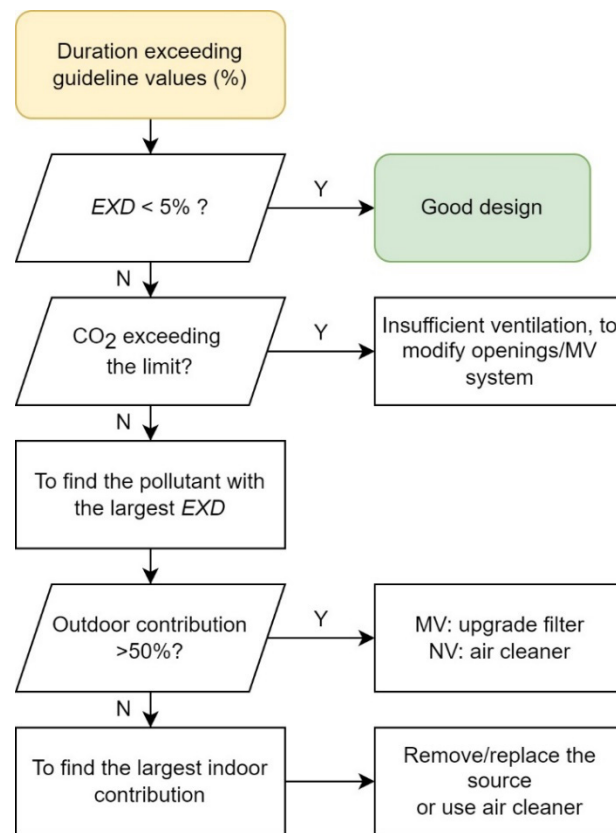


**Figure 3.** The diagnosis flow of the i-IAQ toolbox to deliver suggestions to improve the design. Y: yes; N: no; *EXD*: the duration exceeding the guideline values; MV: mechanical ventilation; NV: natural ventilation.

- When the *EXD* of six air pollutants all less than 5%, it indicates that the current design has achieved the set guidelines, and the toolbox outputs “good design” and finishes the diagnosis flow. Otherwise, the priority of air pollutant diagnosis is given to  $\text{CO}_2$ , because  $\text{CO}_2$  is an indicator of whether the air change rate is adequate to remove human bio-effluents.
- If  $EXD_{\text{CO}_2} > 5\%$ , the toolbox delivers a message indicating insufficient ventilation of the designed building and a suggestion to modify building openings or the mechanical ventilation rate to increase the air change rate. Then, the diagnosis flow finishes and waits for the simulation results of a modified design.
- Otherwise, the toolbox selects the pollutant with the largest *EXD* as the analyzing target. The contribution of outdoor pollution intrusion into the room *i* is calculated by

$$\text{Outdoor contribution } i = \text{average} \left( \frac{Q_{out,i} \eta_i p_i C_{out}}{V_i \times u_i} \right) \times 100\% \quad (13)$$

A value larger than 50% indicates that outdoor intrusion is the major contributor to build up indoor air pollutant levels and should, thus, be prioritized for improvement. The suggestions could include upgrading air filters in the mechanical ventilation system (if it exists) and deploying air cleaners inside the room. The diagnosis flow ends afterwards.

- Otherwise, the toolbox sorts out the largest *E* from those selected from the indoor source/sink database for the target air pollutant. Then, a message containing the name

of the source of the largest contribution is delivered, as well as a suggestion to remove or replace the source and to deploy air cleaners inside the room. Finally, the *Diagnosis* module finishes.

### 3. Development of the Toolbox

The i-IAQ toolbox was developed using MATLAB App Designer 2021a (The MathWorks, Inc., Natick, MA, USA) based on the principles described in Section 2. The App Designer can develop a straightforward user interface with the powerful matrix operations of MATLAB. As observed from Figure 4, the main user interface of the i-IAQ toolbox contains the following four tabs: the building, the ventilation, the pollution source, and the concentration, which are in accordance with the four modules described in Section 2.1.

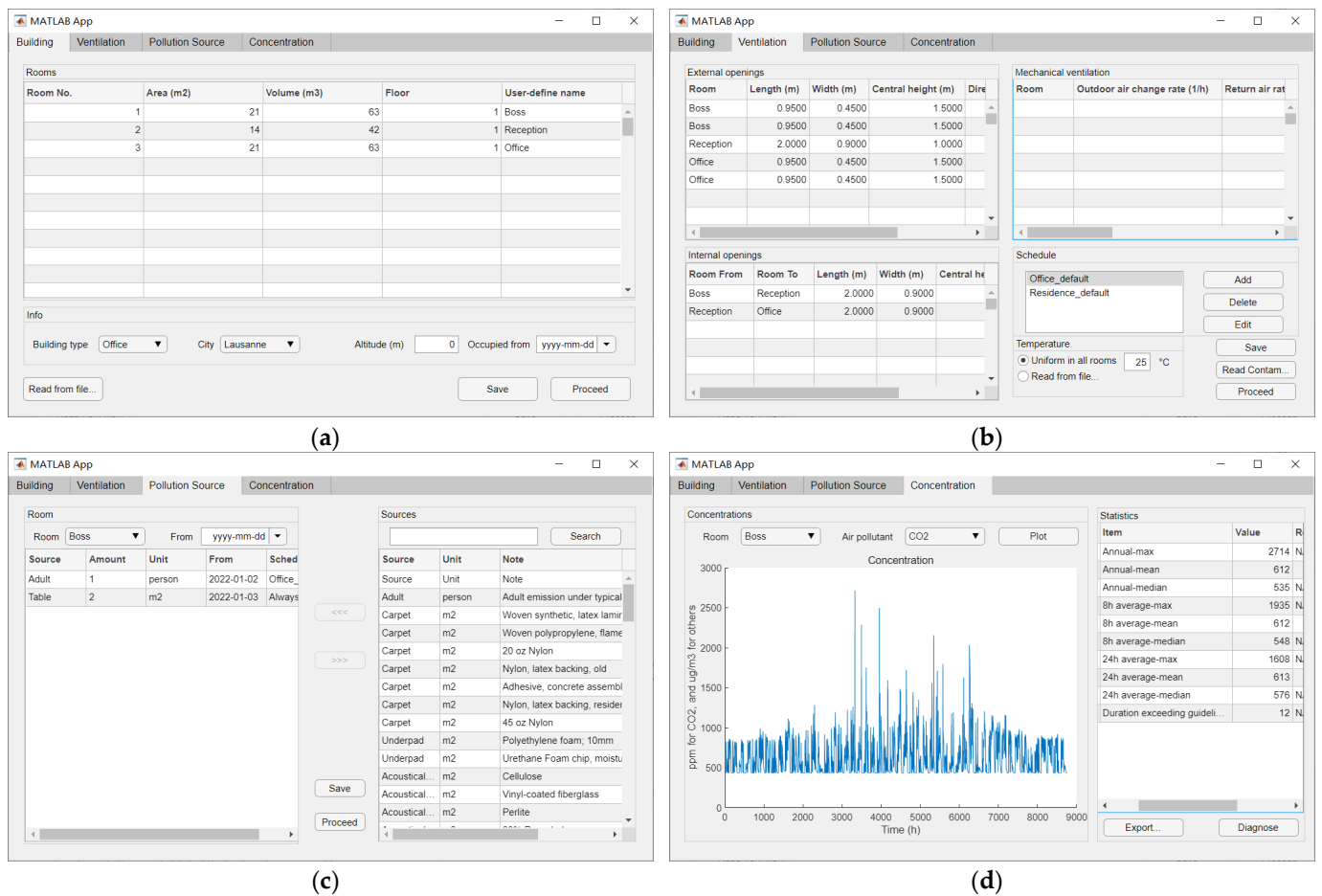


**Figure 4.** User interface design of the i-IAQ toolbox containing (a) building tab; (b) opening tab; (c) pollution source tab; and (d) concentration tab.

The building tab aims to collect basic building information. Users can directly input the number, area, volume, floor, and name of each room in the table, and define building type, city, altitude, and the start date of occupancy.

The ventilation tab receives information regarding the simulation of building ventilation and infiltration. Users can input the length, width, height, and direction of external openings for each room, as well as the size of internal openings between rooms. There is also a table to collect inputs regarding mechanical ventilation, including outdoor air delivery rate and filtration efficiency for each air pollutant. Operation schedule of openings and mechanical ventilation is important to capture the variation in building ventilation. Users can define and edit weekly schedules in the “schedule” panel of this tab, by inputting the start and end hours of window/door opening and mechanical ventilation running in

each day of a week. Then, users can assign the schedule of each opening and mechanical ventilation by selecting from the defined ones. Temperature also plays an essential role in airflow simulation (Equation (5)). In the ventilation tab, users can select to assign a uniform temperature in all rooms, or to read time-series temperature data from an external file. For the temperature file, users need to prepare an  $m \times N$  matrix, where  $m$  is the total simulation hours, 8760, and  $N$  is the number of rooms. The time stamp of the first data row should be in accordance with the start data of the building being occupied.

In the pollution source tab, users can select indoor sources/sinks from the database for each room and define the number, starting date, and schedule of each added source/sink.

Finally, in the concentration tab, users can visualize the plot of each air pollutant in each room, whereas the statistical results are presented in the adjacent table. When users press the “export . . .” button, the time-series concentrations of six air pollutants and their statistics in the selected room will be exported. The *Diagnosis* module starts to run following the scheme shown in Figure 3 after the “diagnose” button is pressed. The toolbox pops up a message box (Figure 5a) describing the detected issue in the selected room and corresponding suggestions to modify the design. In addition, a bar chart (Figure 5b) is shown to illustrate the relative contributions of outdoor intrusion and each indoor source, where air pollutants with  $EXD > 5\%$  are emphasized with bold black edges.

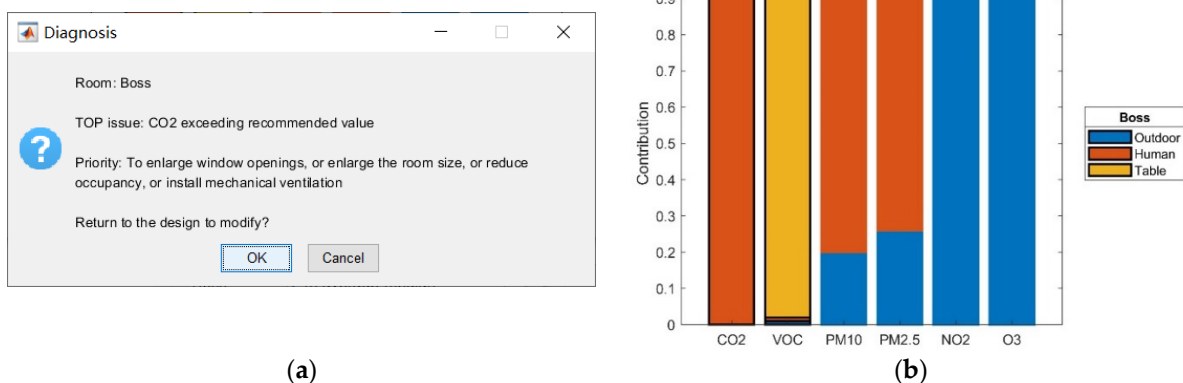


**Figure 5.** An example of the output of the diagnosis function of the i-IAQ toolbox containing (a) a message box describing the top issue detected in the selected room and corresponding suggestions; and (b) a bar chart illustrating contributions of outdoor intrusion and indoor sources to the indoor air pollutant level.

It is worth mentioning that the toolbox is compatible to read outputs from commonly used design software. This is the case for Rhino/Grasshopper (Robert McNeel & Associates, Seattle, WA, USA) by which users can select target building/rooms, calculate the floor area and volume of each room, collect the length, width, height, and direction of each opening, and export the collected data in a *.csv* file. Afterwards, users can import the file by the “read from file . . .” button in the building tab, after which the information will automatically fill the tables of rooms, external openings, and internal openings. Similarly, users who would like to perform building ventilation simulation in the CONTAM software can also run a CONTAM transient simulation of the target building for a year, export airflow results of each flow path, and store them in a folder. Additionally, users need to include in the folder a *.csv* file containing an  $N \times X$  matrix to specify the belonging of each flow path to each room, where  $N$  and  $X$  is the number of rooms and flow paths, respectively. Afterwards, the users can press the “read contam . . .” button in the ventilation tab to import the folder to the toolbox. Then, the toolbox will calculate the airflow network by summing up airflows via flow paths between each two rooms.

#### 4. Validation of the Toolbox

To validate the accuracy of the i-IAQ toolbox, we conducted a case study in a residential building. The concentrations of the six air pollutants were measured continuously for one week, during which the building characteristics and occupant schedule were also collected. Then, the simulation results from the i-IAQ toolbox on the building were compared with the measurements to elucidate the accuracy of the toolbox. Details are presented hereinafter.

##### 4.1. The Case Study

We performed the case study in a 41.6 m<sup>2</sup> residential building on the ground floor located in Fribourg, Switzerland, renovated in July 2021. As shown in Figure 6, the apartment had a 28 m<sup>2</sup> living room (including dining and kitchen), a 10.6 m<sup>2</sup> bedroom and a 3 m<sup>2</sup> bathroom. The living room had two external doors, one external window, and two internal doors connected with the bedroom and bathroom. The bedroom also had one additional door accessible to the outside space, and the bathroom was equipped with an external window. Regarding major indoor sources, the living room was furnished with three tables, four chairs, one cabinet, and one monitor screen, whereas cooking was also a potent and intermittent source. Sources in the bedroom included a bed, a cabinet, a table, a chair, and a monitor screen. The apartment was normally occupied by two adults and one child. There was a main road located in the west of the apartment at a distance of 50 m, and a railway track in the south at 50 m, when the apartment was surrounded by a park with trees to reduce the traffic noise.

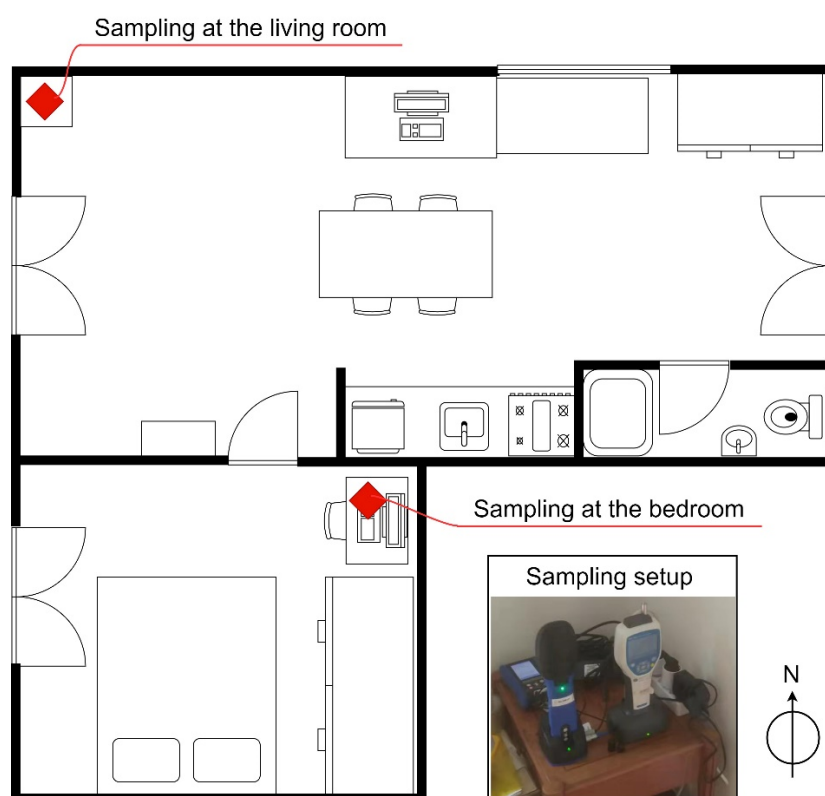


**Figure 6.** The layout of the apartment for case study and the setup for continuous monitoring of indoor air pollutant levels.

We conducted on-site continuous measurements of indoor air pollutants in the target building for a week from 3 May 2022 to 10 May 2022. We deployed two sampling stations located in the living room and bedroom, respectively (Figure 6). The sampling stations were located at a height of 1.0–1.3 m above the floor, and the locations aimed to not interfere with the daily life of the occupants. Each sampling station was equipped

with two instruments recording at a 10-min interval, including one gas sensing probe (AdvancedSensePro with a DS-II probe, Graywolf Sensing Solutions, LLC, Shelton, CT, USA) measuring real-time CO<sub>2</sub> (resolution: 1 ppm; drift: <20 ppm/year), TVOC (resolution: 2.5 µg/m<sup>3</sup>; drift: <25 µg/m<sup>3</sup>/day), NO<sub>2</sub> (resolution: 20 µg/m<sup>3</sup>; drift: 10%/year), and O<sub>3</sub> (resolution: 20 µg/m<sup>3</sup>; drift: 10%/6 months); and one optical particle counter (HPCC 6+, Beckman Coulter, Inc., Brea, CA, USA) measuring real-time particle concentrations. The particle counter measured number concentrations segregated into five size bins, including 0.3–0.5 µm, 0.5–1.0 µm, 1.0–2.0 µm, 2.0–5.0 µm, and 5.0–10 µm. For number-to-mass conversion, we assumed spherical particles with 1.0 g/cm<sup>3</sup> density and constant mass-weighted size distribution within each size bin [83]. The PM<sub>10</sub> and PM<sub>2.5</sub> concentrations were approximated by summing up particle mass of 0.3–10 µm and 0.3–2.0 µm, respectively. All instruments went through factory calibration less than 6 months before the measurement. We implemented side-by-side measurements prior to the case study to mutually correct the disparity between the instruments.

During the case study, we asked the occupants to record the status of window/door openings, occupant number, and specific time of cooking and cleaning events. Afterwards, we input the schedule records, together with the building characteristics, openings, and indoor sources/sinks to the i-IAQ toolbox, to perform IAQ simulation in the case building.

#### 4.2. Validation of the Simulation

Comparisons between the simulation results from the i-IAQ toolbox and the on-site measurement are shown in Figure 7. As observed in Figure 7a, measured CO<sub>2</sub> concentration inside the bedroom regularly fluctuated within 420–1000 ppm, owing to the variation in ventilation and occupant number of the building. The simulation results from the i-IAQ toolbox successfully caught the variation trend of the measured data and generally agreed well with the time-series measured CO<sub>2</sub> values. It demonstrates that the i-IAQ toolbox is reliable to simulate building ventilation and infiltration.

For quantitative comparisons for air pollutant levels, we calculated average simulated and measured concentrations of six air pollutants in the sampled rooms during the case-study week and compared them in Figure 7b. It can be clearly observed that the disparities between the simulated and measured data were within 20% for CO<sub>2</sub>, PM<sub>10</sub>, PM<sub>2.5</sub>, and O<sub>3</sub> in two rooms, indicating good accuracy of the i-IAQ predicting indoor air pollutant levels. For TVOC and NO<sub>2</sub>, the gap between simulation and measurement, however, was relatively large; the i-IAQ toolbox underestimated the concentrations by 3–4 times relative to the measured data. The disparity could be owing to the following three reasons: (1) the toolbox underestimated the indoor source strength of the pollutants. This could particularly be the case for TVOC, since there are many sporadic but strong TVOC sources, such as perfume and sanitizer, which may have not been covered by the indoor source database of the toolbox. (2) The outdoor air pollutant level surrounding the case building was higher than that recorded at the ambient stations. Particularly for TVOC and NO<sub>2</sub> that are easily influenced by local emissions, such as traffic and industry site, using ambient station data to approximate local surrounding air pollution may introduce bias to the simulation results. (3) The accuracy issue of the measurement instrument and deployment. The TVOC sensor had a resolution of 2.5 µg/m<sup>3</sup> and a potential drift of up to 25 µg/m<sup>3</sup> per day, which may cause considerable uncertainty to the measured data. Similarly, the resolution of the NO<sub>2</sub> sensor was 20 µg/m<sup>3</sup>, which was close to the measured average value (24 and 28 µg/m<sup>3</sup>). The deployment of the sampling stations might also introduce bias to the measurement, as they measured only at one point of each room. Although the stations were able to capture the variations in air pollutant levels (Figure 7a), owing to the non-uniformity of air distribution in the sampled rooms, we expected a discrepancy between the measured values and simulation based on the well-mixed assumption. Potential solutions and future work tackling the bias caused by these three assumptions are discussed hereinafter in Section 5.

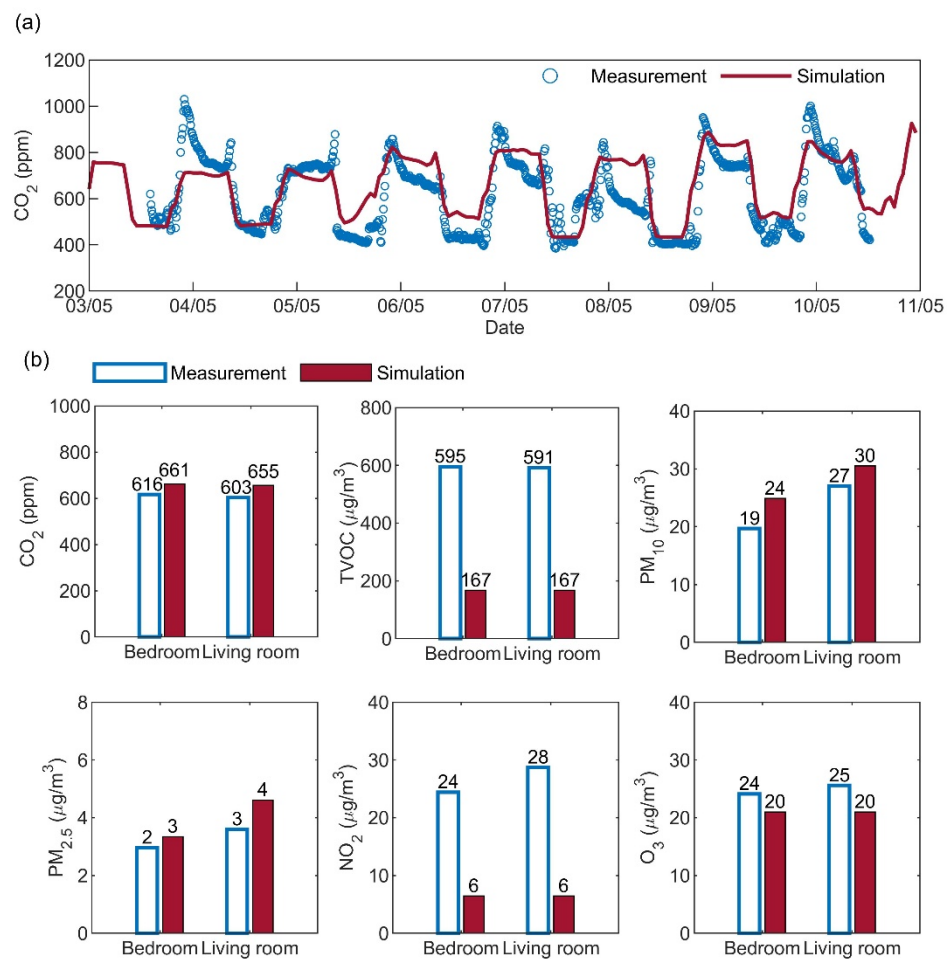


**Figure 7.** Comparisons between the simulation results from the i-IAQ toolbox and the on-site measurement in terms of (a) time-series CO<sub>2</sub> concentration in the bedroom, and (b) average concentrations of CO<sub>2</sub>, TVOC, PM<sub>10</sub>, PM<sub>2.5</sub>, NO<sub>2</sub>, and O<sub>3</sub> in the bedroom and living room during the case-study week.

In conclusion, through a validation case study in a residential building, the i-IAQ toolbox has demonstrated reliability in simulating building ventilation and infiltration, and good accuracy in predicting indoor air pollutant levels.

## 5. Discussion

As described above, based on the mass balance law and multizone modelling and benefiting from the comprehensive indoor/outdoor database, the i-IAQ toolbox is able to reliably predict IAQ and offer diagnosis and suggestions accordingly. The toolbox also has the features of straightforward interface, automatic diagnosis, high prediction accuracy, and compatibility with outputs from widely used design software. These characteristics enable the toolbox to potentially pave a way towards novel and cost-effective IAQ control, and more holistic and quantitative healthy building design, compared to the traditional post-intervention IAQ control strategies. Additionally, in comparison with the existing IAQ prediction tools [50–54], the i-IAQ toolbox has covered a comprehensive air pollutant matrix to better represent IAQ and to propose suggestions for design modification. However, there are several opportunities for improvement of the i-IAQ toolbox. Future work is expected to focus on, but not limited to, the following directions.

One of the priorities should be given to enriching the indoor source/sink database. The toolbox should collect the strengths of indoor sources and sinks from the literature on a regular basis, especially the most recent ones considering the evolution of building

materials, furniture, and other emerging sources/sinks. Similarly, the ambient pollution database requires improvement both in terms of refinement and breadth (increase the number of stations, cities, and countries). The refinement means that in addition to data from ambient stations, the toolbox needs to collect ambient pollution data on a smaller scale (city or community), which can better represent outdoor pollution surrounding a target building. It requires input from high-geological-resolution mapping of air quality in urban environments, which is a trend in the field of smart and healthy cities [84–86]. Future work should also perform more case studies with the i-IAQ toolbox to further validate and enhance the accuracy of the toolbox. It is recommended to measure indoor air pollutant levels at multiple room locations with high-grade instruments or standard passive sampling methods to ensure the reliability of the measurements. These three directions are in accordance with the potential reasons causing the disparities between simulation and measurement data, as discussed in Section 4.2. The i-IAQ toolbox will be made open-accessible after improvements from the three aforementioned perspectives.

To further improve the accuracy of the simulation results from the i-IAQ toolbox, future work should also consider refined zone settings in multizone modelling. Currently, the toolbox sets one room in a building as one zone in the modelling. The setting may be appropriate for residential buildings with relatively small rooms, but not for large spaces in commercial buildings, because large spaces tend to have large gradients of pressure and air pollutant distributions. Hence, it is recommended to discretize large-space rooms into several zones, of which the discretization method and criteria merit further investigations to ensure both accuracy and efficiency. Improving the air pollutant emission model can also enhance the accuracy of the i-IAQ toolbox. For instance, the toolbox currently adopts empirical models to describe TVOC emissions from building materials and furniture. Future work could integrate a mechanism model based on mass transfer to simulate TVOC emissions [87], by which the influence of temperature and humidity on TVOC emissions could also be considered [88]. In addition, regarding the compatibility of the i-IAQ toolbox, currently, the toolbox can only communicate with widely used design software, such as Rhino/Grasshopper and CONTAM, in a simple and one-way approach by reading outputs from them. Future work can consider developing more effective communications between the i-IAQ toolbox and the software, such as creating an i-IAQ plug-in for the software. Moreover, mutual data exchanges between the toolbox and software may enable automatic optimization of the building design [89,90].

## 6. Conclusions

IAQ is an inevitable factor that should be considered in healthy building design. This paper proposes to integrate IAQ prediction into healthy building design by developing a simulation toolbox, i-IAQ, using MATLAB App Designer. Within the i-IAQ, users can define characteristics of designed buildings and openings, and select potential pollutant sources from the pollution database. Afterwards, the toolbox can simulate indoor levels of CO<sub>2</sub>, TVOC, PM<sub>10</sub>, PM<sub>2.5</sub>, NO<sub>2</sub>, and O<sub>3</sub> after occupancy. The toolbox is also capable of offering diagnosis and suggestions for the design based on the simulation results. The reliability of the i-IAQ toolbox was validated by a case study in a residential building. The paper outcomes have the potential to pave a way towards novel and cost-effective IAQ control, and more holistic healthy building design. Future work directions include the following: to enrich and refine indoor/outdoor pollutant databases, to perform more validation case studies and to enhance the accuracy and compatibility of the toolbox.

**Author Contributions:** Conceptualization, S.Y.; methodology, S.Y.; software, S.Y., S.D.M. and S.A.M.; validation, S.Y.; formal analysis, S.Y.; writing—original draft preparation, S.Y.; writing—review and editing, S.Y., S.D.M., S.A.M. and D.L.; supervision, D.L.; project administration, S.Y.; funding acquisition, S.Y. All authors have read and agreed to the published version of the manuscript.

**Funding:** This research was funded by the ENAC Innovation Seed Grant from the School of Architecture, Civil and Environmental Engineering (ENAC) at École Polytechnique Fédérale de Lausanne (EPFL), Switzerland.

**Institutional Review Board Statement:** Not applicable.

**Data Availability Statement:** Not applicable.

**Acknowledgments:** The authors would like to thank Charlotte Vandenberghe, Frédéric Dreyer, Eric Meurville, and Thomas Bourgeau for their technical feedback and administrative support during the project that produced this publication.

**Conflicts of Interest:** The authors declare no conflict of interest.

## References

1. Marco, E.; Burgess, S. *Healthy Housing*; Taylor and Francis Inc.: Oxfordshire, UK, 2015; ISBN 9781317542391.
2. Buildings and Health—GSA Sustainable Facilities Tool. Available online: <https://sftool.gov/learn/about/576/buildings-health> (accessed on 19 May 2022).
3. Healthy Buildings and Healthy People: The next Generation of Green Building | U.S. Green Building Council. Available online: <https://www.usgbc.org/articles/healthy-buildings-and-healthy-people-next-generation-green-building> (accessed on 19 May 2022).
4. Licina, D.; Wargocki, P.; Pyke, C.; Altomonte, S. The Future of IEQ in Green Building Certifications. *Build. Cities* **2021**, *2*, 907–927. [[CrossRef](#)]
5. Loftness, V.; Hakkinen, B.; Adan, O.; Nevalainen, A. Elements That Contribute to Healthy Building Design. *Environ. Health Perspect.* **2007**, *115*, 965–970. [[CrossRef](#)] [[PubMed](#)]
6. Engineer, A.; Gualano, R.J.; Crocker, R.L.; Smith, J.L.; Maizes, V.; Weil, A.; Sternberg, E.M. An Integrative Health Framework for Wellbeing in the Built Environment. *Build. Environ.* **2021**, *205*, 108253. [[CrossRef](#)]
7. Gupta, R.; Howard, A. Comparative Evaluation of Measured and Perceived Indoor Environmental Conditions in Naturally and Mechanically Ventilated Office Environments. *Build. Simul.* **2020**, *13*, 1021–1042. [[CrossRef](#)]
8. Elnaklah, R.; Fosas, D.; Natarajan, S. Indoor Environment Quality and Work Performance in “Green” Office Buildings in the Middle East. *Build. Simul.* **2020**, *13*, 1043–1062. [[CrossRef](#)]
9. Spengler, J.D.; Chen, Q. Indoor Air Quality Factors in Designing a Healthy Building. *Annu. Rev. Energy Environ.* **2003**, *25*, 567–600. [[CrossRef](#)]
10. Jones, A.P. Indoor Air Quality and Health. *Atmos. Environ.* **1999**, *33*, 4535–4564. [[CrossRef](#)]
11. Wolkoff, P. Indoor Air Humidity, Air Quality, and Health—An Overview. *Int. J. Hyg. Environ. Health* **2018**, *221*, 376–390. [[CrossRef](#)]
12. Sundell, J. On the History of Indoor Air Quality and Health. *Indoor Air* **2004**, *14*, 51–58. [[CrossRef](#)]
13. Ole Fanger, P. Indoor Air Quality in the 21st Century: Search for Excellence. *Indoor Air* **2000**, *10*, 68–73. [[CrossRef](#)]
14. Wyon, D.P. The Effects of Indoor Air Quality on Performance and Productivity. *Indoor Air* **2004**, *14*, 92–101. [[CrossRef](#)] [[PubMed](#)]
15. Allen, J.G.; MacNaughton, P.; Satish, U.; Santanam, S.; Vallarino, J.; Spengler, J.D. Associations of Cognitive Function Scores with Carbon Dioxide, Ventilation, and Volatile Organic Compound Exposures in Office Workers: A Controlled Exposure Study of Green and Conventional Office Environments. *Environ. Health Perspect.* **2016**, *124*, 805–812. [[CrossRef](#)] [[PubMed](#)]
16. Du, B.; Tandoc, M.C.; Mack, M.L.; Siegel, J.A. Indoor CO<sub>2</sub> Concentrations and Cognitive Function: A Critical Review. *Indoor Air* **2020**, *30*, 1067–1082. [[CrossRef](#)] [[PubMed](#)]
17. Satish, U.; Mendell, M.J.; Shekhar, K.; Hotchi, T.; Sullivan, D.; Streufert, S.; Fisk, W.J. Is CO<sub>2</sub> an Indoor Pollutant? Direct Effects of Low-to-Moderate CO<sub>2</sub> Concentrations on Human Decision-Making Performance. *Environ. Health Perspect.* **2012**, *120*, 1671–1677. [[CrossRef](#)]
18. Apte, M.G.; Fisk, W.J.; Daisey, J.M. Associations Between Indoor CO<sub>2</sub> Concentrations and Sick Building Syndrome Symptoms in U.S. Office Buildings: An Analysis of the 1994–1996 BASE Study Data. *Indoor Air* **2000**, *10*, 246–257. [[CrossRef](#)]
19. Chatzidiakou, L.; Mumovic, D.; Summerfield, A. Is CO<sub>2</sub> a Good Proxy for Indoor Air Quality in Classrooms? Part 1: The Interrelationships between Thermal Conditions, CO<sub>2</sub> Levels, Ventilation Rates and Selected Indoor Pollutants. *Build. Serv. Eng. Res. Technol.* **2015**, *36*, 129–161. [[CrossRef](#)]
20. Turanjanin, V.; Vučićević, B.; Jovanović, M.; Mirkov, N.; Lazović, I. Indoor CO<sub>2</sub> Measurements in Serbian Schools and Ventilation Rate Calculation. *Energy* **2014**, *77*, 290–296. [[CrossRef](#)]
21. Liang, W.; Yang, S.; Yang, X. Long-Term Formaldehyde Emissions from Medium-Density Fiberboard in a Full-Scale Experimental Room: Emission Characteristics and the Effects of Temperature and Humidity. *Environ. Sci. Technol.* **2015**, *49*, 10349–10356. [[CrossRef](#)]
22. Yang, S.; Yang, X.; Licina, D. Emissions of Volatile Organic Compounds from Interior Materials of Vehicles. *Build. Environ.* **2020**, *170*, 106599. [[CrossRef](#)]
23. Yang, S.; Pernot, J.G.; Jörin, C.H.; Niculita-Hirzel, H.; Perret, V.; Licina, D. Energy, Indoor Air Quality, Occupant Behavior, Self-Reported Symptoms and Satisfaction in Energy-Efficient Dwellings in Switzerland. *Build. Environ.* **2020**, *171*, 106618. [[CrossRef](#)]

24. Yang, S.; Perret, V.; Hager Jörin, C.; Niculita-Hirzel, H.; Goyette Pernot, J.; Licina, D. Volatile Organic Compounds in 169 Energy-efficient Dwellings in Switzerland. *Indoor Air* **2020**, *30*, 481–491. [CrossRef] [PubMed]
25. Weschler, C.J. Changes in Indoor Pollutants since the 1950s. *Atmos. Environ.* **2009**, *43*, 153–169. [CrossRef]
26. Aksoy, M. Benzene as a Leukemogenic and Carcinogenic Agent. *Am. J. Ind. Med.* **1985**, *8*, 9–20. [CrossRef]
27. Kandyala, R.; Raghavendra, S.P.; Rajasekharan, S. Xylene: An Overview of Its Health Hazards and Preventive Measures. *J. Oral Maxillofac. Pathol.* **2010**, *14*, 1. [CrossRef]
28. Lou, X.; Sun, Y.; Lv, D.; Yin, Y.; Pei, J.; He, J.; Yang, X.; Cui, X.; Liu, Y.; Norback, D.; et al. A Study on Human Perception in Aircraft Cabins and Its Association with Volatile Organic Compounds. *Build. Environ.* **2022**, *219*, 109167. [CrossRef]
29. International Agency for Research on Cancer. *Outdoor Air Pollution: IARC Monographs on the Evaluation of Carcinogenic Risks to Humans*; International Agency for Research on Cancer: Lyon, France, 2016.
30. Donaldson, K.; Mills, N.; MacNee, W.; Robinson, S.; Newby, D. Role of Inflammation in Cardiopulmonary Health Effects of PM. *Toxicol. Appl. Pharmacol.* **2005**, *207*, 483–488. [CrossRef] [PubMed]
31. Pope, C.A.; Dockery, D.W. Health Effects of Fine Particulate Air Pollution: Lines That Connect. *J. Air Waste Manag. Assoc.* **2012**, *56*, 709–742. [CrossRef]
32. Yang, S.; Beko, G.; Wargocki, P.; Williams, J.; Licina, D. Human Emissions of Size-Resolved Fluorescent Aerosol Particles: Influence of Personal and Environmental Factors. *Environ. Sci. Technol.* **2021**, *55*, 509–518. [CrossRef]
33. You, R.; Cui, W.; Chen, C.; Zhao, B. Measuring the Short-Term Emission Rates of Particles in the “Personal Cloud” with Different Clothes and Activity Intensities in a Sealed Chamber. *Aerosol Air Qual. Res.* **2013**, *13*, 911–921. [CrossRef]
34. Licina, D.; Tian, Y.; Nazaroff, W.W. Emission Rates and the Personal Cloud Effect Associated with Particle Release from the Perihuman Environment. *Indoor Air* **2017**, *27*, 791–802. [CrossRef]
35. Men, Y.; Li, J.; Liu, X.; Li, Y.; Jiang, K.; Luo, Z.; Xiong, R.; Cheng, H.; Tao, S.; Shen, G. Contributions of Internal Emissions to Peaks and Incremental Indoor PM<sub>2.5</sub> in Rural Coal Use Households. *Environ. Pollut.* **2021**, *288*, 117753. [CrossRef] [PubMed]
36. Diapouli, E.; Chaloulakou, A.; Koutrakis, P. Estimating the Concentration of Indoor Particles of Outdoor Origin: A Review. *J. Air Waste Manag. Assoc.* **2013**, *63*, 1113–1129. [CrossRef] [PubMed]
37. Zhao, S.; Liu, S.; Sun, Y.; Liu, Y.; Beazley, R.; Hou, X. Assessing NO<sub>2</sub>-Related Health Effects by Non-Linear and Linear Methods on a National Level. *Sci. Total Environ.* **2020**, *744*, 140909. [CrossRef] [PubMed]
38. Schwartz, J.; Fong, K.; Zanobetti, A. A National Multicity Analysis of the Causal Effect of Local Pollution, NO<sub>2</sub>, and PM<sub>2.5</sub> on Mortality. *Environ. Health Perspect.* **2018**, *126*, 087004. [CrossRef]
39. Lin, W.; Brunekreef, B.; Gehring, U. Meta-Analysis of the Effects of Indoor Nitrogen Dioxide and Gas Cooking on Asthma and Wheeze in Children. *Int. J. Epidemiol.* **2013**, *42*, 1724–1737. [CrossRef]
40. Pandit, S.; Mora Garcia, S.L.; Grassian, V.H. HONO Production from Gypsum Surfaces Following Exposure to NO<sub>2</sub> and HNO<sub>3</sub>: Roles of Relative Humidity and Light Source. *Environ. Sci. Technol.* **2021**, *55*, 9761–9772. [CrossRef]
41. Weschler, C.J. Ozone’s Impact on Public Health: Contributions from Indoor Exposures to Ozone and Products of Ozone-Initiated Chemistry. *Environ. Health Perspect.* **2006**, *114*, 1489–1496. [CrossRef]
42. Ito, K.; De Leon, S.F.; Lippmann, M. Associations between Ozone and Daily Mortality—Analysis and Meta-Analysis. *Epidemiology* **2005**, *16*, 446–457. [CrossRef]
43. Yang, S.; Gao, K.; Yang, X. Volatile Organic Compounds (VOCs) Formation Due to Interactions between Ozone and Skin-Oiled Clothing: Measurements by Extraction-Analysis-Reaction Method. *Build. Environ.* **2016**, *103*, 146–154. [CrossRef]
44. Weschler, C.J. Ozone in Indoor Environments: Concentration and Chemistry. *Indoor Air* **2000**, *10*, 269–288. [CrossRef]
45. Yang, S.; Licina, D.; Weschler, C.J.; Wang, N.; Zannoni, N.; Li, M.; Vanhanen, J.; Langer, S.; Wargocki, P.; Williams, J.; et al. Ozone Initiates Human-Derived Emission of Nanocluster Aerosols. *Environ. Sci. Technol.* **2021**, *55*, 14536–14545. [CrossRef] [PubMed]
46. Zhang, J.; Li, P.J. Ozone in Residential Air: Concentrations, I/O Ratios, Indoor Chemistry, and Exposures. *Indoor Air* **1994**, *4*, 95–105. [CrossRef]
47. Xiang, J.; Weschler, C.J.; Mo, J.; Day, D.; Zhang, J.; Zhang, Y. Ozone, Electrostatic Precipitators, and Particle Number Concentrations: Correlations Observed in a Real Office during Working Hours. *Environ. Sci. Technol.* **2016**, *50*, 10236–10244. [CrossRef] [PubMed]
48. Standard | WELL V2. Available online: <https://v2.wellcertified.com/en/wellv2/overview> (accessed on 19 May 2022).
49. Shen, J.; Krietemeyer, B.; Bartosh, A.; Gao, Z.; Zhang, J. Green Design Studio: A Modular-Based Approach for High-Performance Building Design. *Build. Simul.* **2021**, *14*, 241–268. [CrossRef]
50. Liang, W.; Yang, X.; Chen, F.; Lv, M.; Yang, S. A Pre-Assessment and Control Tool for Indoor Air Quality (PACT-IAQ) Simulation in Actual Buildings. *Procedia Eng.* **2017**, *205*, 219–225. [CrossRef]
51. Chen, F.; Zhang, H.; Chen, X.; Ren, J. Design Method for Interior Decoration Pollution Control of Buildings: Introduction and Application. *Build. Simul.* **2020**, *13*, 637–646. [CrossRef]
52. Lv, M.; Yang, X. Improving Material Selection for Residences Using Volatile Organic Compound Simulation at Design Stage: Field Verifications from a Unique Case Study. *Build. Environ.* **2019**, *157*, 277–283. [CrossRef]
53. D’Amico, A.; Bergonzoni, G.; Pini, A.; Currà, E. BIM for Healthy Buildings: An Integrated Approach of Architectural Design Based on IAQ Prediction. *Sustainability* **2020**, *12*, 10417. [CrossRef]
54. D’Amico, A.; Pini, A.; Zazzini, S.; D’Alessandro, D.; Leuzzi, G.; Currà, E. Modelling VOC Emissions from Building Materials for Healthy Building Design. *Sustainability* **2020**, *13*, 184. [CrossRef]

55. Dogan, T.; Kastner, P. Streamlined CFD Simulation Framework to Generate Wind-Pressure Coefficients on Building Facades for Airflow Network Simulations. *Build. Simul.* **2021**, *14*, 1189–1200. [[CrossRef](#)]
56. Zhang, Y.; Yu, Y.; Kwok, K.C.S.; Yan, F. CFD-Based Analysis of Urban Haze-Fog Dispersion—A Preliminary Study. *Build. Simul.* **2021**, *14*, 365–375. [[CrossRef](#)]
57. Aflaki, A.; Esfandiari, M.; Mohammadi, S. A Review of Numerical Simulation as a Precedence Method for Prediction and Evaluation of Building Ventilation Performance. *Sustainability* **2021**, *13*, 12721. [[CrossRef](#)]
58. Dols, W.S.; Brian, J.P. *CONTAM User Guide and Program Documentation: Version 3.2*; National Institute of Standards and Technology: Gaithersburg, MD, USA, 2020.
59. ASHRAE. *ASHRAE Handbook: Fundamentals*; American Society of Heating, Refrigerating and Air-Conditioning Engineers: Atlanta, GA, USA, 2001.
60. Climate.Onebuilding.Org. Available online: <https://climate.onebuilding.org/default.html> (accessed on 17 May 2022).
61. Data Query NABEL. Available online: <https://www.bafu.admin.ch/bafu/en/home/topics/air/state/data/data-query-nabel.html> (accessed on 17 May 2022).
62. Daily CO<sub>2</sub>. Available online: <https://www.co2.earth/daily-co2> (accessed on 17 May 2022).
63. He, C.; Morawska, L.; Gilbert, D. Particle Deposition Rates in Residential Houses. *Atmos. Environ.* **2005**, *39*, 3891–3899. [[CrossRef](#)]
64. Liu, Q.; Abbatt, J.P.D. Liquid Crystal Display Screens as a Source for Indoor Volatile Organic Compounds. *Proc. Natl. Acad. Sci. USA* **2021**, *118*, e2105067118. [[CrossRef](#)]
65. Yang, S.; Nie, J.; Wei, F.; Yang, X. Removal of Ozone by Carbon Nanotubes/Quartz Fiber Film. *Environ. Sci. Technol.* **2016**, *50*, 9592–9598. [[CrossRef](#)] [[PubMed](#)]
66. Yang, S.; Zhu, Z.; Wei, F.; Yang, X. Enhancement of Formaldehyde Removal by Activated Carbon Fiber via in Situ Growth of Carbon Nanotubes. *Build. Environ.* **2017**, *126*, 27–33. [[CrossRef](#)]
67. Yang, S.; Zhu, Z.; Wei, F.; Yang, X. Carbon Nanotubes/Activated Carbon Fiber Based Air Filter Media for Simultaneous Removal of Particulate Matter and Ozone. *Build. Environ.* **2017**, *125*, 60–66. [[CrossRef](#)]
68. Persily, A.; de Jonge, L. Carbon Dioxide Generation Rates for Building Occupants. *Indoor Air* **2017**, *27*, 868–879. [[CrossRef](#)]
69. Abadie, M.; Blondeau, P. Pandora Database: A Compilation of Indoor Air Pollutant Emissions. *HVAC R. Res.* **2011**, *17*, 602–613. [[CrossRef](#)]
70. Sun, X.; He, J.; Yang, X. Human Breath as a Source of VOCs in the Built Environment, Part II: Concentration Levels, Emission Rates and Factor Analysis. *Build. Environ.* **2017**, *123*, 437–445. [[CrossRef](#)]
71. Yao, M.; Ke, L.; Liu, Y.; Luo, Z.; Zhao, B. Measurement of Ozone Deposition Velocity onto Human Surfaces of Chinese Residents and Estimation of Corresponding Production of Oxidation Products. *Environ. Pollut.* **2020**, *266*, 115215. [[CrossRef](#)] [[PubMed](#)]
72. Gao, N.P.; Niu, J.L. Modeling Particle Dispersion and Deposition in Indoor Environments. *Atmos. Environ.* **2007**, *41*, 3862–3876. [[CrossRef](#)] [[PubMed](#)]
73. He, J.; Zou, Z.; Yang, X. Measuring Whole-Body Volatile Organic Compound Emission by Humans: A Pilot Study Using an Air-Tight Environmental Chamber. *Build. Environ.* **2019**, *153*, 101–109. [[CrossRef](#)]
74. Shi, S.; Zhao, B. Deposition of Indoor Airborne Particles onto Human Body Surfaces: A Modeling Analysis and Manikin-Based Experimental Study. *Aerosol Sci. Technol.* **2013**, *47*, 1363–1373. [[CrossRef](#)]
75. Zhao, Y.; Zhao, B. Emissions of Air Pollutants from Chinese Cooking: A Literature Review. *Build. Simul.* **2018**, *11*, 977–995. [[CrossRef](#)]
76. Mendes, L.; Kangas, A.; Kukko, K.; Mølgaard, B.; Säämänen, A.; Kanerva, T.; Flores Ituarte, I.; Huhtiniemi, M.; Stockmann-Juvala, H.; Partanen, J.; et al. Characterization of Emissions from a Desktop 3D Printer. *J. Ind. Ecol.* **2017**, *21*, S94–S106. [[CrossRef](#)]
77. Won, D.; Shaw, C.Y.; Won, D. *Investigation of Building Materials as VOC Sources in Indoor Air*; National Research Council Canada: Ottawa, ON, Canada, 2004.
78. Weschler, C.J. Roles of the Human Occupant in Indoor Chemistry. *Indoor Air* **2016**, *26*, 6–24. [[CrossRef](#)]
79. Bart, H.; Israel, G.; Marinus, A.K.; André, C.M.R. *Factorization of Matrix and Operator Functions: The State Space Method*; Springer Science & Business Media: Berlin, Germany, 2007.
80. World Health Organization. *WHO Global Air Quality Guidelines: Particulate Matter (PM<sub>2.5</sub> and PM<sub>10</sub>), Ozone, Nitrogen Dioxide, Sulfur Dioxide and Carbon Monoxide*; World Health Organization: Geneva, Switzerland, 2021.
81. Shrubsole, C.; Dimitroulopoulou, S.; Foxall, K.; Gadeberg, B.; Doutsis, A. IAQ Guidelines for Selected Volatile Organic Compounds (VOCs) in the UK. *Build. Environ.* **2019**, *165*, 106382. [[CrossRef](#)]
82. ANSES. *Concentrations de CO<sub>2</sub> Dans l'air Intérieur et Effets Sur La Santé. Avis de l'ANSES. Rapport d'expertise Collective*; French Agency for Food, Environmental and Occupational Health & Safety: Maisons-Alfort, France, 2013.
83. Zhou, J.; Chen, A.; Cao, Q.; Yang, B.; Chang, V.W.C.; Nazaroff, W.W. Particle Exposure during the 2013 Haze in Singapore: Importance of the Built Environment. *Build. Environ.* **2015**, *93*, 14–23. [[CrossRef](#)]
84. Munir, S.; Mayfield, M.; Coca, D.; Jubb, S.A. Structuring an Integrated Air Quality Monitoring Network in Large Urban Areas—Discussing the Purpose, Criteria and Deployment Strategy. *Atmos. Environ. X* **2019**, *2*, 100027. [[CrossRef](#)]
85. Schäfer, K.; Lande, K.; Grimm, H.; Jenniskens, G.; Gijsbers, R.; Ziegler, V.; Hank, M.; Budde, M. High-Resolution Assessment of Air Quality in Urban Areas—A Business Model Perspective. *Atmosphere* **2021**, *12*, 595. [[CrossRef](#)]
86. Belias, E.; Licina, D. Outdoor PM<sub>2.5</sub> Air Filtration: Optimising Indoor Air Quality and Energy. *Build. Cities* **2022**, *3*, 186. [[CrossRef](#)]

87. Liu, Z.; Nicolai, A.; Abadie, M.; Qin, M.; Grunewald, J.; Zhang, J. Development of a Procedure for Estimating the Parameters of Mechanistic VOC Emission Source Models from Chamber Testing Data. *Build. Simul.* **2021**, *14*, 269–282. [[CrossRef](#)]
88. Liang, W.; Lv, M.; Yang, X. Development of a Physics-Based Model for Analyzing Formaldehyde Emissions from Building Material under Coupling Effects of Temperature and Humidity. *Build. Environ.* **2021**, *203*, 108078. [[CrossRef](#)]
89. Zhang, J.; Liu, N.; Wang, S. A Parametric Approach for Performance Optimization of Residential Building Design in Beijing. *Build. Simul.* **2020**, *13*, 223–235. [[CrossRef](#)]
90. Lin, B.; Chen, H.; Liu, Y.; He, Q.; Li, Z. A Preference-Based Multi-Objective Building Performance Optimization Method for Early Design Stage. *Build. Simul.* **2021**, *14*, 477–494. [[CrossRef](#)]